Frequency Dependence of Speckle in Continuous-Wave Ultrasound with Implications for Blood Perfusion Measurements

Tomas Jansson, Rytis Jurkonis, T. Douglas Mast, *Member, IEEE*,
Hans W. Persson, *Member, IEEE*, and Kjell Lindström, *Member, IEEE*

***Abstract*—Speckle in continuous wave (CW) Doppler has previously been found to cause large variations in detected Doppler power in blood perfusion measurements, where a large number of blood vessels are present in the sample volume. This artifact can be suppressed by using a number of simultaneously transmitted frequencies and averaging the detected signals. To optimize the strategy, statistical properties of speckle in CW ultrasound need to be known. This paper presents analysis of the frequency separation necessary to obtain independent values of the received power for CW ultrasound using a simplified mathematical model for insonation of a static, lossless, statistically homogeneous, weakly scattering medium. Specifically, the autocovariance function for received power is derived, which functionally is the square of the (deterministic) autocorrelation function of the effective sample volumes produced by the transducer pair for varying frequencies, at least if a delta correlated medium is assumed. A marginal broadening of the modeled autocovariance functions is expected for insonation of blood. The theory is applicable to any transducer aperture, but has been experimentally verified here with 5-MHz, 6.35-mm circular transducers using an agar phantom containing small, randomly dispersed glass particles. A similar experimental verification of a transducer used in multiple-frequency blood perfusion measurements shows that the model proposed in this paper is plausible for explaining the decorrelation between different channels in such a measurement.**

I. Introduction

CW DOPPLER ultrasound can be used to estimate local blood perfusion changes as one of several methods (e.g., laser Doppler [1], plethysmography [2], and various ultrasound-based methods [3]–[6]).

The first moment of the Doppler power spectrum (i.e., the spectrum obtained after mixing the received and transmitted signals, followed by low-pass filtering) is, under certain conditions, a measure of "true" (capillary) perfusion [7]–[9]. The first moment can be interpreted as the mean velocity times the total power of the spectrum [10]. An estimate of this quantity can be obtained by applying a linear filter with amplitude function $A(f) = \sqrt{f}$ to the mixed and low-pass filtered signal, followed by squaring and temporal averaging. This is identical to the processing employed in laser Doppler instruments [6], [11], [12]. As this is the only filter used (i.e., no wall filter is present), the method is vulnerable to movement artifacts just as laser Doppler measurements. This problem can be reduced by rigid mounting of the Doppler probe onto the skin. The effect of muscle tonus [13] has not yet been investigated but appears to be small for the regions of interest, as the signal remains low during periods of occlusion.

As the scattered power is not proportional to the number of red blood cells, only relative changes in perfusion can be observed using this technique. Further, two perfusion values obtained at two different locations are not directly comparable as two different vascular situations have been investigated, but perfusion changes over time can be tracked (assuming no other changes in hemodynamic characteristics known to affect the scattered signal intensity during this time [44]). Examples include detection of decreased perfusion in an index finger after the subject smoked one cigarette [9] and reactive hyperaemia [8]. Thus, potential application areas of the technique are studies of perfusion changes in extremities and parenchymal organs in clinical practice or experimental settings after stress provocations or delivery of (vasoactive) drugs.

For long observation times, it has been noted that the perfusion signal fluctuates significantly [12]. Because entirely different values were obtained by shifting the transmitted frequency only slightly (50 kHz or about 5% of the transmitted frequency), it was assumed that these variations did not reflect true perfusion changes but were a result of interference, i.e., speckle. This was also verified in a later study [14].

To reduce variability over time, several averaging strategies are possible, namely spatial (multiple sample volumes, multiple transducers), temporal (averaging of the signal over time), and frequency domain (multiple transmit frequencies, each used for detection in separate channels). The two former techniques obviously decrease either spatial or temporal resolution. The multi-frequency method was suggested and analyzed by Eriksson *et al.* [15]. Four

Manuscript received November 30, 1999; accepted January 9, 2002. SSF (The Swedish Foundation for Strategic Research, project CORTECH), TFR (The Swedish Research Council for Engineering Sciences), the Johnson Foundation, and the ELFA Foundation are thanked for their financial support.

T. Jansson, H. W. Persson, and K. Lindström are with the Department of Electrical Measurements, Lund University, SE-221 00 Lund, Sweden (e-mail: tomas.jansson@elmat.lth.se).

R. Jurkonis is with the Department of Theoretical Radioengineering, Kaunas University of Technology, Studentu st. 50, LT-3031 Kaunas, Lithuania.

T. D. Mast was with the Applied Research Laboratory, The Pennsylvania State University, University Park, PA 16802. Current address: Ethicon Endo-Surgery, Cincinnati, OH 45242.

simultaneously transmitted frequencies all gave different perfusion estimates; the mean was more stable over time. The four frequencies, spaced in 50-kHz increments around 10 MHz, were chosen heuristically by noting a periodicity in the frequency response at the receiver when the transducer was applied to the calf of the subject.

Properties of speckle have been extensively studied for ultrasound imaging [16]–[18]. The speckle can be reduced either by changing the position of the aperture [19], [20] or by altering the transmitted frequency [21], similar to the proposed multi-frequency technique described previously (frequency compounding). The latter strategy was adapted from optics where multicolor processing was used for decreasing speckle noise contrast in laser images. The frequency separations necessary to achieve uncorrelated images to be superimposed was first analyzed by George and Jain [22]–[24]. Although a similar problem, the properties of speckle in the CW ultrasound case seem not to have been investigated. This is presumably because CW ultrasound is generally used in Doppler measurements on larger vessels, and Doppler speckle does not obscure the diagnostic information to the same degree as speckle in ultrasound imaging. The term "Doppler speckle" often refers to noise within a sonogram (spectrogram), even though this noise is mainly a result of the large variance produced by the fast Fourier transform (FFT) estimator [25]. Here, "Doppler speckle" refers to observed variations of the total power of the Doppler spectrum when a collection of randomly ordered vessels are probed and the transmit frequency is altered [14]. Fluctuations in estimated perfusion, caused by such variations of the Doppler spectrum, are the motivation of the present investigation.

The aim of this investigation is to provide a basic understanding of the speckle phenomenon observed in multi-frequency blood perfusion measurements and, specifically, to suggest a method to choose the frequencies properly in a multi-frequency system for a given transducer configuration. However, as a starting point, the analysis will be limited to the static case: statistical properties of the received power from a random inhomogeneous medium containing independent scattering objects, insonated with CW ultrasound, will be investigated. Specifically, an expression will be derived for the autocovariance function $C_P(f_0, f_1)$ of the power in the received signal, which will also be verified experimentally. The validity of this model for a moving medium such as blood, or in other words, to explain variations in the Doppler signal described previously, will also be discussed.

II. Theory

Speckle is an interference phenomenon and is the result of the coherent summation of a large number of scattered waves with random phase over the transducer face. The situation investigated here is described by a transmitter emitting CW ultrasound and a receiver, angled relative to the transmitter, so that a sample volume is formed from which echoes are received. To analyze the speckle effect for this configuration, the sample volume is considered to contain small (i.e., much smaller than a wavelength), weakly scattering, randomly dispersed particles. Because the sample volume extends for many wavelengths, the phase of the returning echoes will be uniformly distributed on the interval $[0, 2\pi]$.

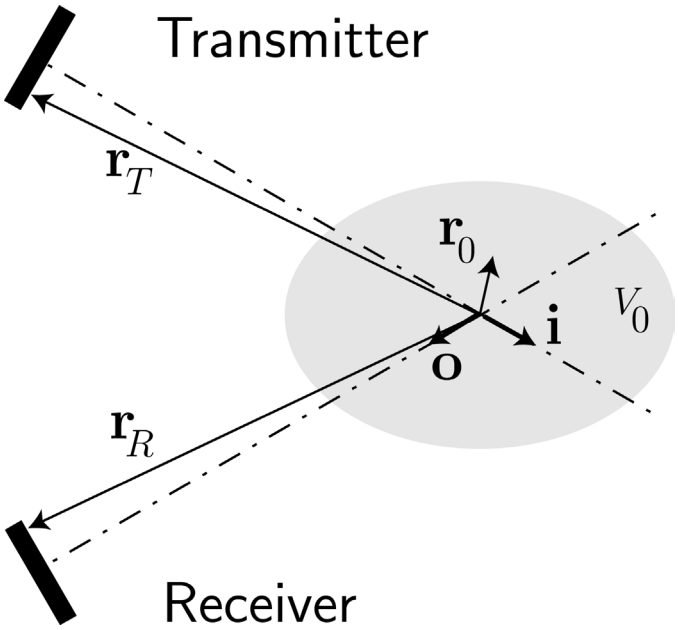

Fig. 1. Geometry of the CW setup with vectors as used in the theory part.

An inhomogeneous medium, such as one with randomly dispersed particles, can be treated as a continuous fluid with compressibility and density variations γ_κ and γ_ρ [26] defined as:

$$\gamma_\kappa = \frac{\kappa - \kappa_0}{\kappa_0}, \quad \gamma_\rho = \frac{\rho - \rho_0}{\rho}$$

where the local compressibility is κ, and the local density is ρ. The ambient quantities are denoted κ_0 and ρ_0, respectively. Assuming that these variations are sufficiently small for the Born approximation to hold, the scattered pressure p_s at a location $\mathbf{r}$ for the CW case can be written:

$$p_s(\mathbf{r}) = \iiint_{V_0} \Big\{ \gamma_\kappa(\mathbf{r}_0) k^2 p_T(\mathbf{r}_0) g(\mathbf{r} - \mathbf{r}_0) + \nabla_0 \cdot [\gamma_\rho(\mathbf{r}_0) \nabla_0 p_T(\mathbf{r}_0)]\, g(\mathbf{r} - \mathbf{r}_0) \Big\}\, d^3 r_0. \tag{1}$$

Here, k denotes the wave number, p_T is the pressure generated by the transmitter at the point $\mathbf{r}_0$, and g is the Green's function for an unbounded medium:

$$g(\mathbf{r}) = \frac{e^{-ik|\mathbf{r}|}}{4\pi|\mathbf{r}|}.$$

The vectors employed in (1) are drawn schematically in Fig. 1.

For a transducer set in an infinite baffle, the emitted pressure p_T can be written:

$$p_T(\mathbf{r}_0) = C_0 \iint_{A_T} g(\mathbf{r}_0 - \mathbf{r}_T)\, d^2 r_T \tag{2}$$

where C_0 is a constant (assuming that the transducer surface is rigid), and A_T is the active surface of the transducer.

Substituting (2) into (1), integrating by parts, and making use of Green's theorem yields the following expression for the scattered pressure:

$$p_s(\mathbf{r}) = C_1 \iiint_{V_0} g(\mathbf{r} - \mathbf{r}_0)(\gamma_\kappa + \mathbf{i}\cdot\mathbf{o}\gamma_\rho) I_T(\mathbf{r}_0) d^3 r_0. \tag{3}$$

In (3), I_T is the integral from (2), and the constant C_0 is incorporated into C_1. This expression has employed the approximations $|\mathbf{r}_0 - \mathbf{r}_T| \approx |\mathbf{r}_T| - \mathbf{i}\cdot\mathbf{r}_0$ for $|\mathbf{r}_T| \gg |\mathbf{r}_0|$ and $|\mathbf{r} - \mathbf{r}_0| \approx |\mathbf{r}| - \mathbf{o}\cdot\mathbf{r}_0$ for $|\mathbf{r}| \gg |\mathbf{r}_0|$, where $\mathbf{i}$ is a unit vector in the propagation direction of the incident wave and $\mathbf{o}$ is a unit vector in the direction of the field point $\mathbf{r}$.

The received signal N is the scattered pressure integrated over the detector surface A_R:

$$N = C_2 \iint_{A_R} p_s(\mathbf{r}_R) d^2 r_R. \tag{4}$$

The coefficient C_2 includes the effect of the electromechanical transfer function at the frequency employed. By rearranging the integral in (4) after insertion of p_s, the effect of the medium can be separated from that of the transducer configuration:

$$N = C_3 \iiint_{V_0} I_R(\mathbf{r}_0) I_T(\mathbf{r}_0) \gamma(\mathbf{r}_0) d^3 r_0. \tag{5}$$

The medium inhomogeneities are described by the function $\gamma = \gamma_\kappa + \mathbf{i}\cdot\mathbf{o}\gamma_\rho$, and the detector integral I_R is defined analogously to the emitter integral I_T by noting the reciprocity property of the Green's function:

$$I_R(\mathbf{r}_0) = \iint_{A_R} g(\mathbf{r}_0 - \mathbf{r}_R)\, d^2 r_R.$$

Thus, the received signal can be represented as a phasor that is the coherent sum of the contributions from each scattering object, where the real part of N corresponds to the measured acoustic pressure. For a static case, this phasor is naturally dependent on the frequency employed, through the wave number used in the emitter and detector integrals. It is also dependent on the orientation of the transducers, as indicated by the product of the emitter and detector integrals.

This is a general result, but, to study the frequency dependence of speckle, a correlation function can be formed as the expected value of the product $N(f_0)N^*(f_1)$ [27], where all other parameters are assumed constant. The asterisk refers to complex conjugation, and the average is over an ensemble of volumes of a medium fulfilling the conditions stated previously. The correlation function can be written:

$$\begin{aligned} R(f_0, f_1) = C_4 \int_{V_0}\int_{V_1} \Lambda(f_0, \mathbf{r}_0)\Lambda^*(f_1, \mathbf{r}_1) \\ \langle \gamma(\mathbf{r}_0)\gamma^*(\mathbf{r}_1)\rangle d^3 r_0 d^3 r_1. \end{aligned} \tag{6}$$

Here, $\Lambda(f, \mathbf{r})$ is the resulting sensitivity at location $\mathbf{r}$ when the frequency f is used (i.e., the product of the emitter and detector integrals). The brackets indicate expected values.

For random media that are statistically homogeneous, $\langle \gamma(\mathbf{r_0})\gamma^*(\mathbf{r_1})\rangle$ is dependent only on the difference between $\mathbf{r_0}$ and $\mathbf{r_1}$, so that the autocorrelation function of the inhomogeneity γ can be written:

$$B_\gamma(\mathbf{r_0} - \mathbf{r_1}) = \langle \gamma(\mathbf{r_0})\gamma^*(\mathbf{r_1})\rangle.$$

Now, if the structure of the medium is such that the correlation length of the medium is small compared with the wavelength (as if it contains small, randomly and sparsely dispersed particles), B_γ can be set equal to the Dirac delta function [28]. Then, the autocorrelation function becomes:

$$R(f_0, f_1) = C_5 \iiint_{V_0} \Lambda(f_0, \mathbf{r}_0)\Lambda^*(f_1, \mathbf{r}_0) d^3 r_0. \tag{7}$$

(essentially, the autocorrelation of the (deterministic) system function). This is similar to the findings of other investigators analyzing this limiting case of speckle [17], [23]. However, here the result is not naturally interpreted in terms of a "point spread function," even though $\Lambda(f_0, \mathbf{r}_0)$ can be said in some sense to resemble this, as it determines the response of the system to a point target in the field.

Eq. (7) is now the autocorrelation function for the received signal in terms of a complex phasor N. It is usually more convenient to study the received power, which is related to the complex phasor as $P = N\,N^*$. The autocorrelation function for received power is given in terms of N as:

$$R_P(f_0, f_1) = \langle N(f_0)N(f_1)N^*(f_0)N^*(f_1)\rangle. \tag{8}$$

Using a general result from statistics, this expected value of a product of four random variables can be expanded as:

$$\begin{aligned} R_P(f_0, f_1) = \langle N(f_0)N^*(f_0)\rangle \cdot \langle N(f_1)N^*(f_1)\rangle \\ + \langle N(f_0)N^*(f_1)\rangle \cdot \langle N(f_1)N^*(f_0)\rangle, \end{aligned} \tag{9}$$

as outlined in [23]. The second term is equivalent to $|R(f_0, f_1)|^2$, and the received power autocorrelation can be written as:

$$R_P(f_0, f_1) = \langle P(f_0)\rangle \cdot \langle P(f_1)\rangle + |R(f_0, f_1)|^2. \tag{10}$$

By definition [27], the autocovariance of the received power, $C_P(f_0, f_1)$ is then:

$$C_P(f_0, f_1) = |R(f_0, f_1)|^2. \tag{11}$$

Any frequency dependence of the transducers (such as included in C_2) will cancel if C_P is normalized to obtain the correlation coefficient [27]:

$$r = \frac{C_P}{\sqrt{\sigma_{f_0}^2 \sigma_{f_1}^2}} \tag{12}$$

where $\sigma_{f_i}^2$ is the variance of the power obtained at f_i, $i = 0$ or 1.

Notable is that the covariance function is dependent not only on the difference of the frequencies, but also on their absolute values.

The emitter and detector integrals, I_T and I_R, respectively, were evaluated for these experiments using the impulse response method. The time domain solution for the integral in (2) has been shown by Oberhettinger [29] to be the aperture impulse response for the velocity potential at the field point $\mathbf{r}$. For a circular aperture, the impulse response can be calculated analytically using the so-called equidistant line method [30] for the three common types of boundary conditions [31], [32]. In the theory developed previously, an infinite rigid baffle was assumed, which was employed in these calculations. Strictly, this is not the case in the experimental situation, but the choice of boundary condition is not critical for a transducer with a diameter extending over many wavelengths and in the region where $\Lambda(f, \mathbf{r})$ is significant [33]. The pressure at the field point is then obtained by evaluating the Fourier transform of the impulse response [34].

To calculate the beam function $\Lambda(f, \mathbf{r})$, it is necessary that the two transducers share the same coordinate system. Consider a single transducer placed in a Cartesian coordinate system with the transducer face in the xy-plane and the acoustic axis being aligned with the z-axis. For a two-transducer setup similar to the one in Fig. 2, the common coordinate system (x', y', z') is found via the transformation

$$\begin{bmatrix} x' \\ y' \\ z' \end{bmatrix} = \begin{bmatrix} \theta & 90 & 90-\theta \\ 90 & 0 & 90 \\ 90+\theta & 90 & \theta \end{bmatrix} \begin{bmatrix} x - x_0 \\ y - y_0 \\ z - z_0 \end{bmatrix} \tag{13}$$

where

$$\begin{bmatrix} x_0 \\ y_0 \\ z_0 \end{bmatrix} = \begin{bmatrix} R \sin\theta \\ 0 \\ R(1 - \cos\theta) \end{bmatrix} \tag{14}$$

is the point of the aperture center when the beams intersect with an angle 2θ on the z-axis at distance R, as defined in Fig. 2.

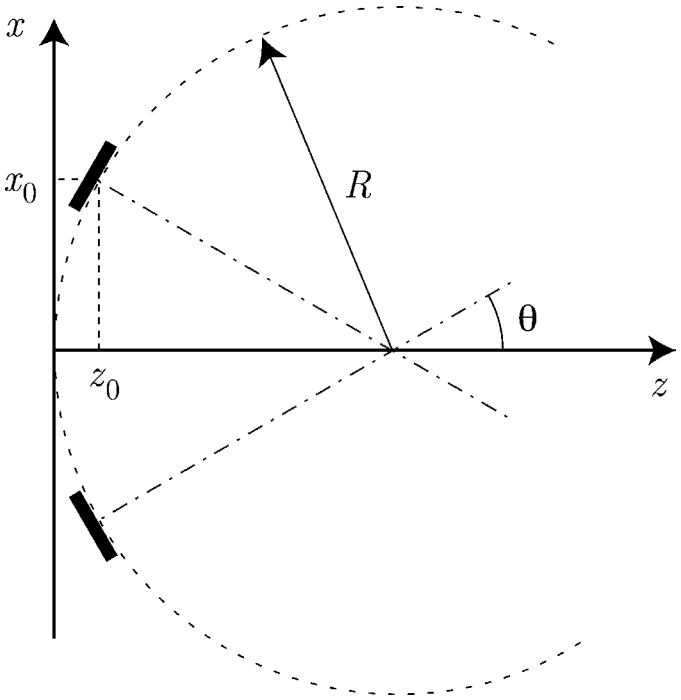

Fig. 2. Geometry of the two transducer setup for calculation of the beam function $\Lambda(f, \mathbf{r})$.

III. Materials and Methods

For experimental verification of the theory, an agar phantom was produced that fulfilled the requirements stated previously, i.e., it contained small, randomly dispersed scattering objects. The phantom had a cylindrical shape with a diameter of 34 mm and a length of 120 mm. The phantom was molded to a holder that fit a stepper motor fixture, allowing uncorrelated measurements at different angles and cross sections.

The procedure for manufacturing the phantom is described elsewhere [35]. For these experiments, 4 g of glass spheres with mean diameter of 93 μm (type A2429 glass, Potters Industries, Valley Forge, PA) were added per liter agar solution to serve as scattering sources, corresponding to a number density of 5.37 spheres/mm^3. However, here, sodium benzoate was used for preservation instead of formaldehyde. The phantom was checked for flaws and uniform sphere distribution using a commercial ultrasound scanner equipped with a broadband 5- to 12-MHz probe.

Two circular 5-MHz transducers were used to verify the theoretical calculations just described. The transducers were manufactured in-house and had a physical diameter of 6.35 mm. They were fitted in a specially designed holder so that their acoustic axes could be angled 30°, 45°, and 60° to each other. To check for non-uniformities in the produced fields, a 0.2-mm hydrophone (Precision Acoustics, Dorchester, UK) was used to scan the transducers in a plane parallel to the transducer face (distance = 1 mm) and in a plane including the acoustic axis. The measured areas were 8 mm × 8 mm (0.1-mm steps) and 9 mm × 40 mm (0.2-mm steps), respectively.

From these measurements, the effective radiating diameter was calculated by noting the distance to the boundary between the Fresnel and Fraunhofer regions (theoretically found at a^2/λ, where a is the transducer radius and λ is

the wavelength). This was found by fitting a fourth-order polynomial to the measured amplitude along the acoustic axis from the point of the last minimum, extending into the far field, and finding the maximum of the polynomial. The effective diameter was then used in the theoretical calculations of the beams that were then used in the autocovariance function.

Four different transducer configurations, denoted subsequently as (a)–(d), were analyzed both theoretically and experimentally. Configurations (a)–(c) had angles of 30°, 45°, and 60° between the acoustic axes ($\theta = 15, 22.5, 30$ in Fig. 2). The beams intersected 30 mm from the transducer faces ($R = 30$ mm in Fig. 2), which was approximately 7 to 8 mm beyond the boundary between the Fresnel and Fraunhofer regions in water for these particular transducers. In configuration (d), the angle between the acoustic axes was 60°, but the beams intersected only 12 mm from the transducer faces; this was done to investigate whether the theory would hold also in the nearfield case.

The sample volumes produced by the transducer pair were measured in a plane including the acoustic axes of the transducers. This was achieved by emitting a 4.9-MHz, 50-cycle, 8-V peak-to-peak burst on the emitter, moving a steel tip in the field, and detecting the amplitude on the receiver (the burst mode was employed to avoid any standing waves between the emitter and the tip or its holder). The tip was made from a 2-mm diameter steel rod, tapered so that the end of the rod had a flat, round surface of 0.2-mm diameter. For each transducer configuration (i.e., for the different angles and the nearfield case), these measurements were compared with the theoretical sample volume $\Lambda(f, \mathbf{r})$ evaluated in the measured plane.

The phantom to be scanned was mounted in a stepping motor fixture that allowed the phantom to be rotated and translated vertically. The movements of the phantom were controlled using the same software as for data collection (LabView, National Instruments, Austin, TX). The phantom was scanned in a water tank where the walls had been covered with a sound-absorbing material. The material was a rubber-based, in-house prepared material with a documented reflection coefficient of <0.01.

For the experiments, a continuous 5-V peak-to-peak voltage was applied to the transducer acting as a transmitter. The frequency synthesizer (Hewlett Packard HP3325A, Andover, MA) was controlled via GPIB from a standard personal computer so that the frequency could be altered automatically. The receiving transducer was connected via an amplifier with 40-dB gain over 0.5 to 20 MHz (Panametrics 5676, Waltham, MA) to an ac-coupled digitizing oscilloscope (Tektronix TDS 360, Wilsonville, OR). A time window corresponding to roughly five wavelengths was transferred via GPIB to the computer, where the amplitude of the acquired waveform was determined.

To find the translations of the phantom necessary to obtain uncorrelated intensities, initial experiments were performed using a single frequency (4.9 MHz), and the covariance function for received power versus translated angle and distance was calculated using setup (c). The resulting correlation functions were found to approach 0 after 4° and 2.8 mm, respectively. Based on this, measurements were made at 6° rotational increments and 5-mm vertical translations to ensure uncorrelated measurements, which meant that a total of 300 independent positions was measured.

For each position, amplitude values were collected around the center frequency of the transducers (4.85 MHz), starting from 4.7 to 5.0 MHz with 5-kHz increments.

The correlation function for power was finally calculated from the square of the measured amplitude values using standard routines in MATLAB (The MathWorks, Natick, MA).

The beam functions $\Lambda(f, \mathbf{r})$ were calculated in a rectangular volume of dimensions $8 \times 8 \times 20$ mm, centered on the intersection of the acoustic axes of the transducers, with 0.25-mm steps. The impulse responses were calculated using a sampling rate of 256 MHz.

IV. Results

To compare the theory with experimental results, it was necessary to verify that the transducers produced symmetric fields with minimal or no drop out on the active surface. The hydrophone scan of the plane parallel to the transducer face in Fig. 3 (left panels) reveals that the soldering point on the silver surface of the piezo-ceramic is noticeable, as has been seen in nearfield measurements such as this [36]. A scan of the plane aligned with the arrows in Fig. 3 shows, however, that this has little effect on the overall beam pattern (Fig. 3; right panels). The spot producing higher intensity on transducer two can be seen to cause a somewhat asymmetrical beam in the far field.

A comparison between theoretical and measured sample volumes in the plane, including the acoustic axes of the transducers, are shown in Fig. 4. The asymmetry of the beams, noted previously, causes the experimental sample volumes not to match the theoretical volumes perfectly.

The theoretical normalized covariance functions for the sample volumes corresponding to the four investigated transducer configurations are shown in Fig. 5 to 8. Basically, these are the results from evaluating (12) with the geometries given as in configurations (a) to (d). Note that the diameter of the transducer used in the calculations is not the physical diameter, but rather the effective radiating diameter as determined from the measured distance to the boundary between the Fresnel and Fraunhofer regions.

The experimental results are shown in the same figures as dashed lines. The correlation coefficient was calculated for each vertical translation (i.e., a group of 60 measurements). The average of the resulting five functions and the standard deviation divided by $\sqrt{5}$ are plotted in Fig. 5 to 8. Normalization of the covariance function using (12) cancels any variations caused by bandwidth limitations of the transducers or to increased scattering from small particles at higher frequencies. The only limiting factor is that the

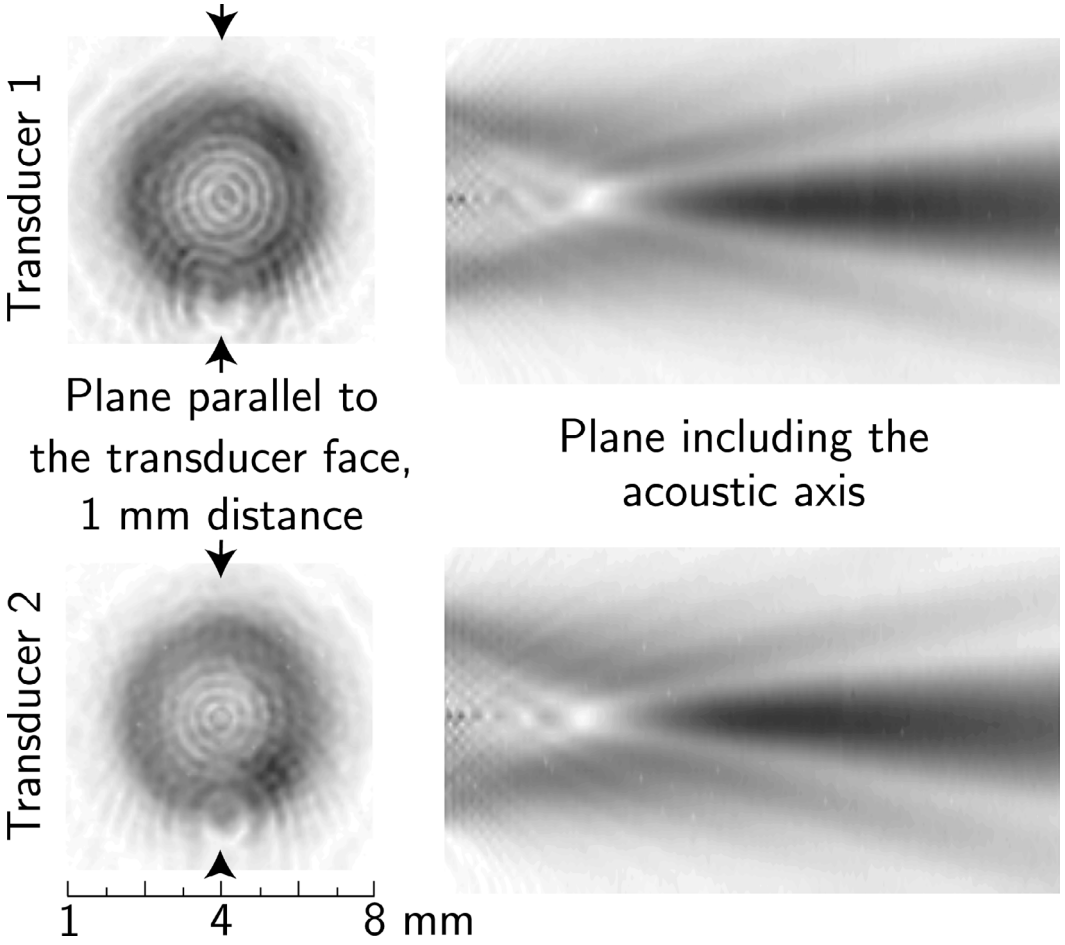

Fig. 3. Measured fields from the two transducers used in the experiments. As the peak positive pressure rises, the image darkens. Upper panels: transducer 1; lower panels: transducer 2. Transducer 1 acted as transmitter in the experiments. The horizontal scale for the view including the acoustic axis has been compressed 250%.

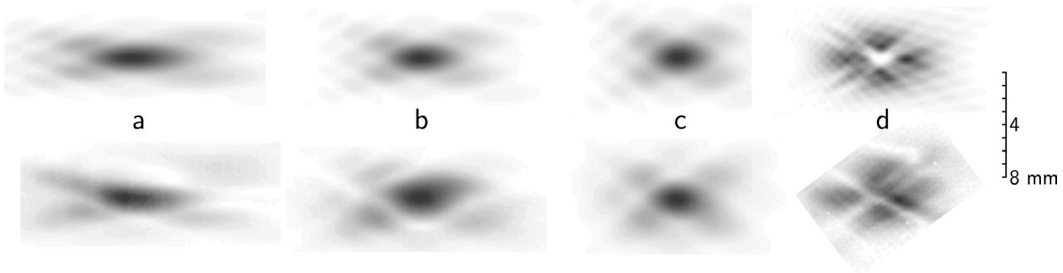

Fig. 4. Comparison of experimental versus theoretical sensitivity in the slice of the sample volume that includes the acoustic axes for the four experimental setups (a) to (d). Darker shading reflects higher sensitivity. The upper row is the theoretical result, and the lower row is experimentally determined.

measurements should be made within the bandwidth of the transducers so that the signal-to-noise ratio (SNR) remains reasonably high. It is interesting to note that SNR values of the speckle, defined as the mean amplitude divided by the standard deviation, are 1.938, 1.956, 1.954, and 1.901 for the four measurements, compared with the number 1.913 predicted for uncorrelated speckle by other investigators [16], [17].

V. Discussion

The present model, based on the autocorrelation of the beam function, appears to predict the frequency separation necessary for uncorrelated speckle adequately. Deviations between the modeled and experimental decorrelation results are most likely caused by discrepancies between the experimental and theoretical sample volumes (Fig. 4), an issue that will be discussed subsequently.

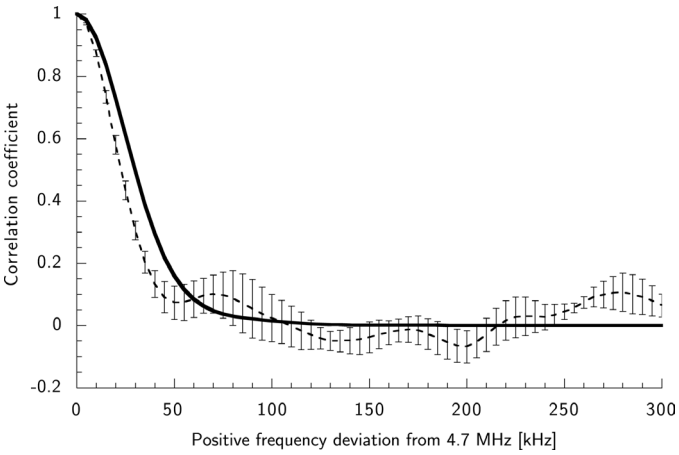

Fig. 5. Normalized autocovariance function of the intensity for varying frequency. Transmitted frequency = 4.7 to 5.0 MHz. Angle between transducers = 30°. Solid line: theory. Dashed line with error bars are means (plus and minus one standard error) from experimental data.

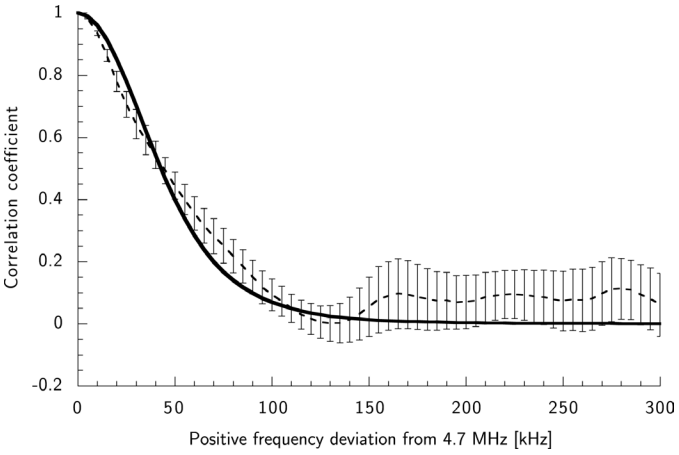

Fig. 6. Normalized autocovariance function of the intensity for varying frequency. Transmitted frequency = 4.7 to 5.0 MHz. Angle between transducers = 45°. Solid line: theory. Dashed line with error bars are means (plus and minus one standard error) from experimental data.

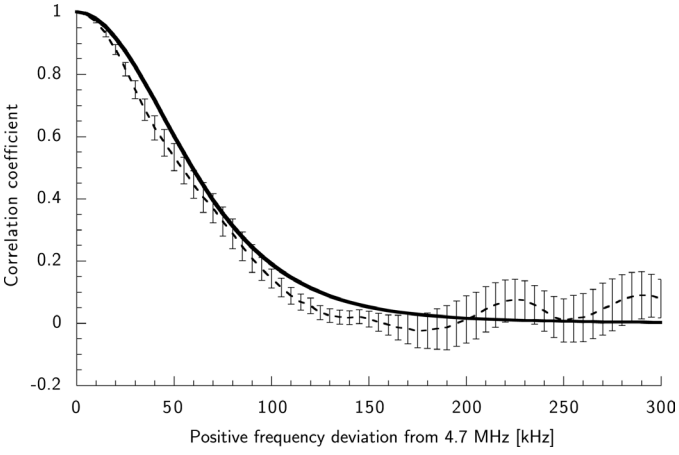

Fig. 7. Normalized autocovariance function of the intensity for varying frequency. Transmitted frequency = 4.7 to 5.0 MHz. Angle between transducers = 60°. Solid line: theory. Dashed line with error bars are means (plus and minus one standard error) from experimental data.

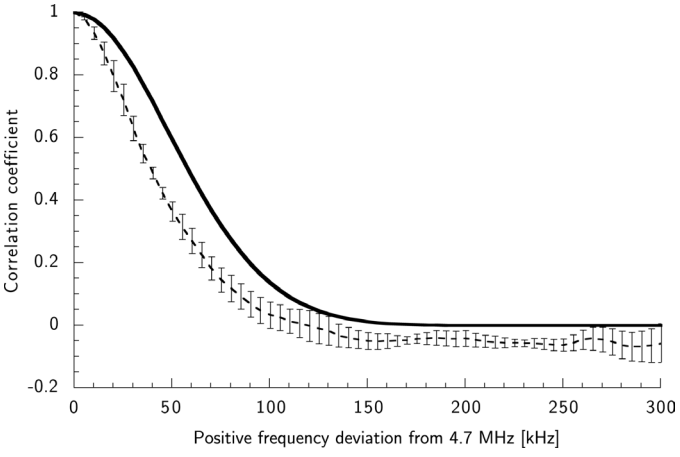

Fig. 8. Normalized autocovariance function of the intensity for varying frequency. Transmitted frequency = 4.7 to 5.0 MHz. Angle between transducers = 60°, but only 12 mm to the intersection of the acoustic axes. Solid line: theory. Dashed line with error bars are means (plus and minus one standard error) from experimental data.

Attenuation is not included in the model, but could easily be included in the beam functions, either by noting the mean distance to the transducer face from each field point or by introducing a complex wave number. However, as the attenuation of the agar medium is rather low ($0.032\,f^{1.84}$ dB/cm; [35]), this is believed to be a minor effect here (Fig. 4). In any case, the effect of attenuation would probably be to broaden the covariance function (see subsequent discussion).

The SNR of the speckle was found to be somewhat higher than that expected for fully developed, uncorrelated speckle, suggesting that a somewhat different form of speckle may be encountered here. This effect could, however, be a result of the limited SNR of the measurement in itself, which was about 60, taken as the mean square detected amplitude divided by the mean square noise amplitude.

Another explanation for the measured speckle SNR could be the particle size. The mean diameter of the glass spheres was stated to be 93 μm, but 10% of the glass spheres had a diameter exceeding 138 μm (based on the manufacturer's specifications). This radius is sufficiently large ($ka = 1.4$ for $a = 69$ μm) that some of the spheres clearly failed to meet the Rayleigh scattering criterion $ka \ll 1$ [37]. A consequence of larger particles in the sample volume is an increase of the SNR [38]. As for the influence of particle size on the covariance function, larger particles would also be expected to have a broadening effect [Eq. (6)].

The number of spheres (/mm^3) corresponds to an average number of 63, 45, 37, and 200 spheres within the 6 dB limits of the sample volumes in the four cases (a) to (d). As few as 10 scatterers per resolution cell, however, have been shown sufficient to produce developed speckle [38], [39].

Another consequence of the relatively large glass spheres is that the angular dependence of the scattered

field is no longer constant as a function of frequency. This means that as the scattering angle is larger in the part of the sample volume close to the transducer and smaller in the part farther away, the scattering phase and amplitude will change differently in these regions when the frequency is altered. Consequently, this is a factor that would tend to make the decorrelation faster. However, the angle differences are small (approximately 6° at the −6 dB limits of the sample volume for cases (a) to (c) and approximately 24° for case (d)). The frequency range for significant covariance functions is also small (approximately 150 kHz).

To assess the effect of finite scatterer size on the present results, the scattered field for a single glass sphere (90-μm diameter) was computed using physical parameters provided by the manufacturer [35], an exact series solution [40], and a small scatterer approximation [26, Eq. (8.2.19)]. The difference between the exact and the approximate solution was found to be relatively large at 4.7 MHz, but this difference only affects the interpretation of the exact size and position of the glass sphere, as the sphere is stationary. The only differences significant to the covariance function are relative changes in the frequency dependence of the computed phase and amplitude over the angles encountered in the different sample volumes.

A comparison indicates that the computed approximate amplitude increases about 3% more than the exact solution over the scattering angles 102° to 126° (case (d)) when the frequency is increased 150 kHz from 4.7 MHz. The phase increases less than 0.1° more. In cases (a) through (c), the corresponding numbers are less than 0.7%, and less than 0.01° for the scattering angles in those cases. Thus, it appears that any effect on the measured covariance functions arising from non-ideal characteristics of the glass spheres is very small.

The coarseness of the spatial and temporal discretization in calculating the beam functions has a very small effect on the resulting covariance function, as long as a sufficient number of points is included. Covariance functions calculated with 0.5-mm steps differ <0.02% (maximum at any point) from those presented here (using 0.25-mm steps between field points). A similar result was obtained for a 25% coarser temporal discretization when calculating the impulse responses. A random spatial grid, with 0.4-mm mean distance between points, changed the covariance functions <0.4%.

From the results of the decorrelation for angular and vertical translation, it is interesting to note that the criterion of one-half aperture length for decorrelated speckle, as predicted by other investigators, holds also in this CW case (the transducer radius, 2.7 mm, corresponds to approximately 5° at a 30-mm distance).

After this discussion of the results, how can an intuitive understanding of the significance of the covariance function be provided? Clearly, the covariance function is directly dependent on the size and form of the sample volume, as the beams at two frequencies are integrated over space (7). Therefore, it seems reasonable to assume that the frequency shift needed to decouple the intensity is associated with the difference in path length from various parts of the sample volume. When the transmitted frequency is altered, the number of wavelengths that fit into a ray from a point on the emitter, via the scattering object, and back to the receiver, will change. For one frequency, waves traveling along two different rays may be in phase. For a large enough frequency shift, they may be out of phase and cancel each other. Presumably, this first occurs where the pathlengths are the longest (i.e., at the edges of the sample volume). Also, from this, it can be seen that a large sample volume needs a relatively smaller frequency shift for this to occur.

A more formal way of examining the effect of sample volume size is to consider a wavespace formulation of the autocorrelation function (7). Under the assumption of a statistically homogeneous medium, the convolution theorem allows (6) to be rewritten in the form:

$$R(f_0, f_1) = C_6 \int_{V_k} \hat{\Lambda}(f_0, \mathbf{k})\, \hat{\Lambda}^*(f_1, \mathbf{k})\, \hat{B}_\gamma(\mathbf{k})\, d^3\, k \tag{15}$$

where a beam function $\hat{\Lambda}$ denotes the three-dimensional spatial Fourier transform of the real-space sensitivity function Λ and $\hat{B}_\gamma(\mathbf{k})$ is the power spectrum of the medium variations γ. If the medium variations are nearly constant over the spatial-frequency range, where the wavespace beam functions $\hat{\Lambda}$ are significant, then (15) can be approximated as:

$$R(f_0, f_1) \approx C_6\, \hat{B}_\gamma \left(\frac{\pi(f_0 + f_1)}{c} (\mathbf{i} - \mathbf{o}) \right) \int_{V_k} \hat{\Lambda}(f_0, \mathbf{k})\, \hat{\Lambda}^*(f_1, \mathbf{k})\, d^3\, k, \tag{16}$$

which is a wavespace analog of (8). Because wide coverage in real space corresponds to narrow beam functions in wavespace, the assumption that $\hat{B}_\gamma$ is constant (or similarly, the assumption that the medium autocorrelation function $B_\gamma(\mathbf{r}_0 - \mathbf{r}_1)$ is a Dirac delta function) leads to better approximations when the sample volume is large [41]. Also, because the central wavespace location of each beam function depends directly on the frequency employed, the wavespace autocorrelation function (16) provides another explanation for the decorrelation that occurs with small frequency shifts and large sample volumes. For narrowly concentrated wavespace beam functions, a small frequency shift can result in a wide relative separation, so that the autocorrelation function defined by (16) becomes increasingly narrow for larger sample volumes. For the limiting case of an infinite sample volume (a "one-transducer" CW-Doppler system, which could be made using a very high dynamic range in the receiving stage), the corresponding wavespace beam function would be the narrowest [41], and, consequently, only a small frequency shift would be needed to decouple the intensity of the detected signal.

In summary, a simple explanation of the phenomenon may be that the effective size and proportions of the sample volume are the determinants of the frequency shift

needed for decorrelation—the longer the path differences in the sample volume, the smaller the frequency shift.

From the results in this study, one can also see a relationship between sample volume size and the frequency needed for decorrelation. For instance, consider the sample volume of case (c). The main peak of the sample volume is about 3 mm in the range direction (6-dB limit). Therefore, the two-way path difference is roughly 6 mm for rays via the front and back of the sample volume, respectively. For a 180° phase shift over this distance, a "wavelength" of 12 mm is needed, which, in water, corresponds to a frequency (or frequency increase) of 125 kHz. This is consistent with the findings in the experimental and theoretical study (Fig. 7). As the angle between the transducers decreases, and thereby the sample volume lengthens (Fig. 5 to 8), the covariance function becomes increasingly narrow, consistent with the reasoning presented previously.

The purpose of setup (d) was to determine whether the theory is also applicable for nearfield configurations. Based on Fig. 8, one may be led to believe that this is not the case. However, this is probably an effect of the discrepancy of the experimental sample volume relative to the theory (Fig. 4). The reason for the relationships not to hold in the nearfield is the angular dependence of scattering caused by density variations. However, Ueda and Ichikawa [42] have found that this effect is only appreciable as close to the transducer as one radius of the transducer, for a density contrast of 2.7 in their case. In the experiments presented here, the density contrast is $2.489/1.015 \approx 2.5$ [35]. When considering that the closest part of the sample volume is some 8 mm from the transducer face, the theory would presumably be valid in this case and probably also as close to the transducer as it is practically possible to form a sample volume. When applying these results to blood perfusion measurements, the density contrast would be for blood cells to surrounding plasma, where this ratio is, of course, much smaller.

The theoretical model presented in this study holds for a medium containing small, weak scattering, randomly dispersed particles. The experiments also show that there is still adequate agreement even if the particles pass the limit to be considered small and have a high compressibility/density contrast. For blood, which is the medium in which this model has its application area, conditions are reversed. Red blood cells are indeed small and weak scattering, but not necessarily randomly dispersed. In fact, blood cells are very densely packed and, therefore, give rise to both coherent and incoherent scattering [43]. The blood cells can, therefore, be said to be neither uncorrelated nor perfectly uncorrelated. Thus, the assumption of B_γ as a Dirac delta function may not hold for blood, and the result will be a broadened covariance function. The size of this effect needs to be further investigated, but can be expected to be small when the correlation length of the medium is small compared with the spread of the beam product $\Lambda(f_0, \mathbf{r}_0)\,\Lambda^*(f_1, \mathbf{r}_0)$. This assumption is most likely to hold for blood, even under varying flow conditions [44], [45].

The question remains whether these results can be applicable to moving blood or, more specifically, to determine uncorrelated frequencies in a multi-frequency system for blood perfusion estimation. In the study by Eriksson *et al.* [15], the perfusion value was estimated as the first moment of the Doppler power spectrum, as obtained after demodulation and low-pass filtering (the power is the same as the power described by the covariance functions). If one considers a large number of blood vessels in the sample volume, instead of a large number of stationary scatterers, it seems plausible that Doppler signals would interfere in the same way as those from stationary scatterers. In other words, the assumption would then be that the scatterers producing the Doppler shift Δf using transmit frequency f_0 would produce (nearly) the same Doppler shift at transmit frequency f_1, but with uncorrelated amplitude (power), provided that the transmit frequencies are chosen in this manner. Naturally, this also assumes that the Doppler shifts are small compared with the width of the covariance function.

The experiment reported in [15] does support the assumption that the frequencies chosen there were uncorrelated, at least for those vessels under investigation. The detected Doppler shifts did not extend beyond 200 Hz (limited by a filter), so the condition of small Doppler shift was also fulfilled. One should, however, avoid jumping to conclusions. A measurement on the glass sphere phantom as described previously, with the same transducer used in the experiments described by Eriksson *et al.*, shows that a frequency separation of nearly 150 kHz is necessary for uncorrelated intensities.

This may be compared with the 50-kHz separation found heuristically by those investigators, which apparently resulted in uncorrelated perfusion values between channels. However, one needs to consider how the Doppler signal was obtained in that case: by mixing the received signal with the transmitted and thus obtaining only the in-phase component of the Doppler signal. Preliminary results show that the covariance function for the squared amplitude of the phasor of the Doppler signal (i.e., as obtained after quadrature demodulation) follows closely the one obtained in the static case described previously [46]. The covariance function for the in-phase component appears from the preliminary experiments to be an oscillating function, with an envelope defined by the covariance function for the phasor magnitude. When employing only the in-phase component, one would seemingly need a smaller frequency shift between channels to obtain independent Doppler signals than predicted by the theory here. However, only slight changes in the shape of the sample volume, for instance as a result of refraction, may cause an uncertainty in estimates of the necessary frequency separation.

In summary, it seems plausible that the model presented here predicts the frequency separations necessary to obtain independent Doppler power in a multi-frequency system used for blood perfusion estimation.

VI. Conclusion

A theoretical model that predicts the necessary frequency shift to obtain independent received power from a random medium in a CW ultrasound setup has been presented. The model correlates well with experimental data and may serve as a prediction for how to choose frequencies in multi-frequency blood perfusion measurements for independent perfusion estimates on each channel.

Acknowledgments

The authors thank Dr. P. Wahlberg, Dr. R. Eriksson, and Prof. A. Lukosevicius for numerous helpful discussions. Prof. R. C. Waag is thanked for kindly supplying the glass spheres used in the experiments. Maria Edholm is acknowledged for designing the measurement system.

References

[1] G. E. Nilsson, "A survey of the laser Doppler technique for measurement of tissue perfusion," *Laser Therapy*, vol. 1, pp. 175–182, 1989.

[2] R. S. C. Cobbold, *Transducers for Medical Measurements: Principles and Applications*. New York: John Wiley & Sons, 1974, pp. 301–306.

[3] D. S. Bell, J. C. Bamber, and R. J. Eckersley, "Segmentation and analysis of colour Doppler images of tumour vasculature," *Ultrasound Med. Biol.*, vol. 21, pp. 635–647, 1995.

[4] J. M. Rubin, R. S. Adler, J. B. Fowlkes, S. Spratt, J. E. Pallister, J.-F. Chen, and P. L. Carson, "Fractional moving blood volume: Estimation with power Doppler US," *Radiology*, vol. 197, pp. 183–190, 1995.

[5] T. R. Porter and J. Gwajg, "Myocardial contrast echocardiography: A new gold standard for perfusion imaging," *Echocardiography*, vol. 18, pp. 79–87, 2001.

[6] T. Jansson, H. W. Persson, and K. Lindström, "Estimation of blood perfusion using ultrasound," *Proc. Inst. Mech. Eng. Part H, J. Eng. Med.*, vol. 213, pp. 91–106, 1999.

[7] C. H. Hertz, "The estimate of blood volume and blood perfusion in tissue," presented at the 4th Eur. Cong. Ultrasound in Medicine, Dubrovnik, May 17–24, 1981.

[8] S. O. Dymling, "Measurement of blood perfusion in tissue using Doppler ultrasound," Ph.D. dissertation, Department of Electrical Measurements, Lund Institute of Technology, 1985.

[9] S. O. Dymling, H. W. Persson, and C. H. Hertz, "Measurements of blood perfusion in tissue using Doppler ultrasound," *Ultrasound Med. Biol.*, vol. 17, pp. 445–452, 1991.

[10] P. Atkinson and J. P. Woodcock, *Doppler Ultrasound and its Use in Clinical Measurement*. London: Academic Press, 1982.

[11] G. E. Nilsson, T. Tenland, and P. Å Öberg, "Evaluation of a laser Doppler flowmeter for measurement of tissue blood flow," *IEEE Trans. Biomed. Eng.*, vol. BME-27, pp. 597–604, 1980.

[12] R. Eriksson, H. W. Persson, S. O. Dymling, and K. Lindström, "Evaluation of Doppler ultrasound for blood perfusion measurement," *Ultrasound Med. Biol.*, vol. 17, pp. 433–444, 1991.

[13] A. Heimdal and H. Torp, "Ultrasound Doppler measurements of low velocity blood flow: Limitations due to clutter signals from vibrating muscles," *IEEE Trans. Ultrason., Ferroelect., Freq. Contr.*, vol. 44, pp. 873–881, 1997.

[14] T. Jansson, H. W. Persson, and K. Lindström, "Evaluation of a multi frequency technique for blood perfusion measurements," in *Proc. IEEE Utrason. Symp.*, vol. 2, pp. 1217–1220, 1996.

[15] R. Eriksson, H. W. Persson, S. O. Dymling, and K. Lindström, "Blood perfusion measurements with multifrequency Doppler ultrasound," *Ultrasound Med. Biol.*, vol. 21, pp. 49–57, 1995.

[16] C. B. Burckhardt, "Speckle in ultrasound B-mode scans," in *IEEE Trans. Sonics Ultrason.*, vol. SU-25, pp. 1–6, 1978.

[17] R. F. Wagner, S. W. Smith, J. M. Sandrik, and H. Lopez, "Statistics of speckle in ultrasound B-scans," *IEEE Trans. Sonics Ultrason.*, vol. SU-30, pp. 156–163, 1983.

[18] W. F. Walker and G. E. Trahey, "The application of K-space in pulse echo ultrasound," *IEEE Trans. Ultrason., Ferroelect., Freq. Contr.*, vol. 45, pp. 541–558, 1998.

[19] G. E. Trahey, S. W. Smith, and O. T. von Ramm, "Speckle pattern correlation with lateral aperture translation: Experimental results and implications for spatial compounding," *IEEE Trans. Ultrason., Ferroelect., Freq. Contr.*, vol. 33, pp. 257–264, 1986.

[20] M. O'Donnell and S. D. Silverstein, "Optimum displacement for compound image generation in medical ultrasound," *IEEE Trans. Ultrason., Ferroelect., Freq. Contr.*, vol. 35, pp. 470–476, 1988.

[21] P. A. Magnin, O. T. von Ramm, and F. L. Thurstone, "Frequency compounding for speckle contrast reduction in phased array images," *Ultrason. Imaging*, vol. 4, pp. 267–281, 1982.

[22] N. George and A. Jain, "Speckle reduction using multiple tones of illumination," *Appl. Opt.*, vol. 12, pp. 1202–1212, 1973.

[23] N. George and A. Jain, "Space and wavelength dependence of speckle intensity," *Appl. Phys.*, vol. 4, pp. 201–212, 1974.

[24] N. George, A. Jain, and R. D. S. Melville, Jr., "Experiments on the space and wavelength dependence of speckle," *Appl. Phys.*, vol. 7, pp. 157–169, 1975.

[25] J. A. Jensen, *Estimation of Blood Velocities Using Ultrasound*, Cambridge, UK: Cambridge University Press, 1996.

[26] P. M. Morse and K. U. Ingard, *Theoretical Acoustics*. New York, NY: McGraw-Hill, 1968.

[27] A. Papoulis, *Probability, Random Variables, and Stochastic Processes*, 3rd ed., New York, NY: McGraw-Hill, 1991.

[28] J.-F. Chen, J. A. Zagzebski, F. Dong, and E. L. Madsen, "Estimating the spatial autocorrelation function for ultrasound scatterers in isotropic media," *Med. Phys.*, vol. 25, pp. 648–655, 1998.

[29] F. Oberhettinger, "On transient solutions of the baffled piston problem," *J. Res. Natl. Bureau Stand. (U.S.)*, vol. 65B, pp. 1–6, 1961.

[30] P. R. Stepanishen, "Transient radiation from pistons in an infinite planar baffle," *J. Acoust. Soc. Amer.*, vol. 49, pp. 1629–1638, 1971.

[31] D. Guyomar and J. Powers, "Boundary effects on transient radiation fields from vibrating surfaces," *J. Acoust. Soc. Amer.*, vol. 77, pp. 907–915, 1985.

[32] J. L. SanEmeterio and L. G. Ullate, "Diffraction impulse response of rectangular transducers," *J. Acoust. Soc. Amer.*, vol. 92, pp. 651–662, 1992.

[33] G. S. Kino, *Acoustic Waves*. Englewood Cliffs, NJ: Prentice-Hall, 1987.

[34] J. C. Lockwood and J. G. Willette, "High-speed method for computing the exact solution for the pressure variations in the nearfield of a baffled piston," *J. Acoust. Soc. Amer.*, vol. 53, pp. 735–741, 1973.

[35] T. T. Jansson, T. D. Mast, and R. C. Waag, "Measurements of differential scattering cross section using a ring transducer," *J. Acoust. Soc. Amer.*, vol. 103, pp. 3169–3179, 1998.

[36] M. Almqvist, A. Holm, T. Jansson, H. W. Persson, and K. Lindström, "High resolution light diffraction tomography: Nearfield measurements of 10 MHz continuous wave ultrasound," *Ultrasonics*, vol. 37, pp. 343–353, 1999.

[37] A. D. Pierce, *Acoustics*. New York, NY: McGraw-Hill, 1981, pp. 425–428.

[38] R. F. Wagner, M. F. Insana, and S. F. Smith, "Fundamental correlation lengths of coherent speckle in medical ultrasound images," *IEEE Trans. Ultrason., Ferroelect., Freq. Contr.*, vol. 35, pp. 34–44, 1988.

[39] E. Jakeman, "Speckle statistics with a small number of scatters," in *Proc. SPIE*, vol. 243, pp. 9–19, 1980.

[40] J. J. Faran, "Sound scattering by solid cylinders and spheres," *J. Acoust. Soc. Amer.*, vol. 23, pp. 405–418, 1951.

[41] T. D. Mast and R. C. Waag, "Wave space resolution in ultrasonic scattering measurements," *J. Acoust. Soc. Amer.*, vol. 98, pp. 3050–3058, 1995.

[42] M. Ueda and H. Ichikawa, "Analysis of an echo signal reflected from a weakly scattering volume by a discrete model of the medium," *J. Acoust. Soc. Amer.*, vol. 70, pp. 1768–1775, 1981.

[43] L. Y. L. Mo and R. S. C. Cobbold, "Theoretical models of ultrasonic scattering in blood," in *Ultrasonic Scattering in Biological*

Tissues. K. K. Shung and G. A. Thieme, Eds. Boca Raton, FL: CRC Press, 1993.
[44] K. K. Shung, G. Cloutier, and C. C. Lim, "The effects of hematocrit, shear rate, and turbulence on ultrasonic Doppler spectrum from blood," *IEEE Trans. Biomed. Eng.*, vol. 39, pp. 462–469, 1992.
[45] B. A. J. Angelsen, "A theoretical study of the scattering of ultrasound from blood," *IEEE Trans. Biomed. Eng.*, vol. 27, pp. 61–67, 1980.
[46] T. Jansson, H. W. Persson, and K. Lindström, "Movement artefact suppression in blood perfusion measurements using a multifrequency technique," *Ultrasound Med. Biol.*, vol. 28, pp. 59–68, 2002.

Tomas Jansson was born in Hagfors, Sweden in 1967. He received the M.Sc. and the Ph.D. degrees in 1993 and 1999, respectively, from Lund University, Lund, Sweden. Part of his Ph.D. studies he spent at the University of Rochester, Rochester, NY, where he was involved in studies of scattering and wavefront distortion for one year.

Since 2000, he has been employed as an assistant professor at the Department of Electrical Measurements, Lund University, and the Department of Biomedical Engineering, Linköping University. His current research interests include measurements of blood flow using various ultrasound techniques, such as continuous wave Doppler, power Doppler, and contrast agents.

Rytis Jurkonis received the B.S. (1994), M.S. (1995), and Ph.D. (2000) degrees in electric engineering from Kaunas University of Technology, Kaunas, Lithuania. Between 1995 and 1996, he worked as a research assistant in the Ultrasound Biomedical Engineering Laboratory. His research interest is in medical ultrasound, dealing with simulations of acoustic wave propagation, diffraction, speed dispersion, and acoustic energy absorption.

T. Douglas Mast (M'98) was born in St. Louis, Missouri in 1965. He received the B.A. degree (Physics and Mathematics) in 1987 from Goshen College and the Ph.D. degree (Acoustics) in 1993 from The Pennsylvania State University.

From 1993 until 1996, he was a postdoctoral research associate with the University of Rochester's Ultrasound Research Laboratory. From 1996 until 2001, he was with the Applied Research Laboratory of The Pennsylvania State University, where he was Research Associate and Assistant Professor of Acoustics. He currently works as Senior Electrical and Computer Engineer for Ethicon Endo-Surgery in Cincinnati, Ohio. His research interests include propagation and scattering in inhomogeneous media, ultrasonic imaging, tissue characterization, and nondestructive testing.

Hans W. Persson (S'77–M'80) received the degrees of M.Sc. and Ph.D. in 1975 and 1980, respectively, from the Lund Institute of Technology, Lund University, Sweden. He worked as a visiting research engineer from 1977 to 1978 at University of Rochester, Rochester, NY. Since then, he has been with Lund Institute of Technology, Department of Electrical, and, in 1999, he was promoted to Professor in Electrical Measurements. His research interests include ultrasound transducer design, ultrasonic field measurements, blood perfusion measurements, acoustic streaming, Doppler vector tomography, noninvasive ultrasonic methods for vascular diagnosis, air-coupled ultrasound, and micromachined ultrasound transducers.

Kjell Lindström (M'89) was born in Gällivare, Sweden in 1942. He received the degrees of M.Sc. and Ph.D. in electrical engineering from Lund Institute of Technology, Lund University, Sweden, in 1966 and 1978, respectively.

From 1971 to 1985, he held a position as Head of the Department of Biomedical Engineering at the Malmö University Hospital. Since 1985, he has held the title of Chair in Electrical Measurements at the Lund Institute of Technology, Lund University, and also serves as Professor in Biomedical Engineering at the Department of Radiology and Physiology, Malmö University Hospital. His research interests center around measurement science and biomedical engineering, especially fundamental aspects of ultrasound technology, Doppler ultrasound, and its application for cardiovascular assessment.